DOI: 10.1021/ma902057f

Macromolecules
ARTICLE

Structure and Properties of Dynamic Rigid Rod-Like Metallo-Supramolecular Polyelectrolytes in Solution

Guntram Schwarz,*[†,▽] Yves Bodenthin,[∥] Thomas Geue,[⊥] Joachim Koetz,[#] and Dirk G. Kurth*[†,‡,§,▽]

[†]*University of Würzburg, Chemical Technology of Advanced Materials, D-97070 Würzburg, Germany,* [‡]*National Institute for Materials Science, 1-1 Namiki, Tsukuba, Ibaraki 305-0044, Japan,* [§]*Fraunhofer-Institut für Silicatforschung ISC, Neunerplatz 2, 97082 Würzburg, Germany,* [∥]*Swiss Light Source, Paul Scherrer Institute, CH-5232 Villigen-PSI, Switzerland,* [⊥]*Laboratory for Neutron Scattering, ETH Zurich and Paul Scherrer Institute, CH-5232 Villigen, Switzerland, and* [#]*University of Potsdam, Institute of Physical and Theoretical Chemistry, D-14476 Potsdam, Germany.* [▽] *Previous address: Max-Planck-Institute of Colloids and Interfaces, D-14424 Golm, Germany.*

Received September 15, 2009; Revised Manuscript Received October 21, 2009

ABSTRACT: Metal-ion-induced self-assembly in aqueous solution of the rigid ligand 1,4-bis(2,2′:6′,2″-terpyridine-4′-yl)benzene (**1**) with $Fe(OAc)_2$ and $Ni(OAc)_2$ is investigated with viscosimetry, SANS, and AFM. Ligand **1** forms extended, rigid-rod like metallo-supramolecular coordination polyelectrolytes (MEPEs) with a molar mass of up to 200 000 g mol^{-1} under the current experimental conditions. The molar mass depends on concentration, stoichiometry, and time. By spin-coating MEPEs on a solid surface, we can image the MEPEs in real space by AFM. Both AFM and SANS confirm the extended rigid-rod-type structure of the MEPEs. As a control experiment, we also studied the flexible ligand 1,3-bis[4′-oxa(2,2′:6′,2″-terpyridinyl)]propane (**2**). Ligand **2** does not form extended macro-assemblies but likely ringlike structures with three to four repeat units. Finally, we present a protocol to control the stoichiometry during self-assembly using conductometry, which is of paramount importance to obtain meaningful and reproducible results.

Introduction

The design of macromolecular structures utilizing inorganic elements adds a new dimension to the field of polymer materials. Coordination numbers and geometries become additional variables to the structure, and metal-ions give access to unusual functions, for example, electrochemical,[1,2] magnetic,[3] thixotropic,[4] self-healing,[5] photophysical,[6,7] or electronic[8] properties that are not accessible through carbon-based polymers with covalent bonds. The potential for these materials can be envisioned if we consider the impact of inorganic solid-state materials on research and technology. Several types of organometallic polymers can be distinguished on the basis of how the metal is integrated in the polymer. Metals can be pendent to or they can be present in the polymer backbone. In coordination polymers, the coordinative bond between the metal and the ligand is an integral part of the backbone.[9,10] Whereas polymers based on kinetically inert transition-metal complexes are readily characterized in solution by means of standard analytical methods, polymers formed by kinetically labile transition-metal complexes have until very recently successfully evaded characterization in solution.[11−13]

For the design of dynamic coordination polymers, the binding constants are the central parameters that determine the kinetic and thermodynamic properties of the assembly. If the interaction is too strong, then the macroassemblies will not be responsive and may precipitate from solution. If the interaction is too weak, then the competition between ligands and solvent molecules for the metal ion will limit the growth of the assemblies. Therefore, in solution, the binding constants have to be of intermediate strength. In general, growth occurs through successive binding steps between the metal ion and two or more ligands, where each event is characterized by a binding constant. The relative strength of the binding constants affects the properties of the metallo-supramolecular assemblies, for example, the relation of molecular weight and stoichiometry. Also ligand design has to be taken into consideration if the structure of the assemblies is under consideration. Under thermodynamic control, flexible ligands form discrete metallomacrocycles, such as rings, of low molecular mass.[14] Rigid ligands, on the other side, cannot form closed structures and thus form extended macromolecular assemblies under the appropriate conditions.

With many transition-metal-ions, terpyridines have the appropriate binding constants to support dynamic macromolecular assemblies. If two terpyridines are linked through covalent back-to-back connection, the pseudo-octahedral coordination geometry enables linear, extended assemblies in aqueous media. The binding constant, K_1, of the initial coordination step of a metal ion, M, and the first ligand, L, is considerably smaller than K_2 of the consecutive coordination step of a second ligand, which constitutes the growth step. The bis-terpyridine complex is, therefore, the preferred species in solution, even in the presence of excess metal ions.[15] Theory of metal-induced self-assembly predicts that in the presence of excess ligand the molecular weight is small and growth of extended assemblies occurs as the stoichiometry, y, that is the metal ion to ligand concentration, approaches 1.[16] On the basis of the first principles of thermodynamics, we anticipate that the mean length increases with concentration.[17]

*Corresponding author. Address: Julius-Maximilians-University Würzburg, Chemical Technology of Advanced Materials, Röntgenring 11, D-97070 Würzburg, Germany. Tel: +49(0)931-31-82157. Fax: +49(0)931-31-82109. E-mail: guntram.schwarz@matsyn.uni-wuerzburg.de.

 Published on Web 11/02/2009

Previously, we have shown that ditopic bis-terpyridines form extended metallo-supramolecular coordination polyelectrolytes (MEPEs) in solution with transition-metal ions such as Fe(II), Ni(II), or Co(II).[18] The positive charge can be utilized to incorporate the MEPEs in various material architectures, including thin films,[18] liquid crystals,[19] or nanostructures.[20] We can make use of the MEPEs in electrochromic coatings[21] or spin-crossover materials.[22] However, because of the dynamic nature, a detailed characterization of the MEPE in solution is missing because the traditional methods of polymer analysis cannot be applied to these systems.

Here we present a first study of the structure of the MEPE based on the rigid ligand 1,4-bis(2,2′:6′,2″-terpyridine-4′-yl)benzene (**1**) in aqueous solution. The flexible ligand 1,3-bis-[4′-oxa(2,2′:6′,2″-terpyridinyl)]propane (**2**) (Scheme 1) is used for control experiments. To adjust the stoichiometry, which has a profound impact on the molecular weight of MEPE, we present a protocol that relies on conductometric control of metal-ion-induced self-assembly. Using small angle neutron scattering (SANS) and viscosimetry, we determine the structure in solution as function of concentration and stoichiometry. In addition, we use atomic force microscopy (AFM) to measure the length of MEPEs on solid surfaces in real space.

Experimental Section

The ditopic ligands 1,4-bis(2,2′:6′2″-terpyridine-4′-yl) benzene (**1**) and 1,3-bis[4′-oxa(2,2′:6′,2″-terpyridinyl)]propane (**2**) were synthesized according to literature procedures.[23,24] Chemicals were purchased from Aldrich and used without further purification. A typical titration procedure for Fe-MEPE is as follows: 25 mg (0.448 mmol) iron powder was dispersed in 15 mL of carefully degassed glacial acetic acid in a volumetric flask. The dispersion was heated under reflux and under argon until the iron powder had completely disappeared and reacted to 77.86 mg (0.448 mmol) $Fe(OAc)_2$, which took ~2 h. In a separate 100 mL two-necked flask equipped with a conductivity sensor, a lower molar quantity of ligand (120 mg, 0.222 mmol) was dissolved in 60 mL of acetic acid solution (75 vol %). The solution containing the freshly synthesized $FeOAc_2$ is cooled to room temperature and titrated to the ligand solution while the conductivity is metered. After each titration, the solution was stirred until the conductivity had settled to a constant value with an accuracy of ± 0.1 μS, which generally took no more than 3 min. Toward the end of the titration (1:1 stoichiometry), the amount added to the solution is gradually reduced to 25 μL. Each addition is accompanied by a corresponding decrease in the conductivity. Because of the small amount that was added, the end point or 1:1 stoichiometry is recognized by the observation that the conductivity does not change for two consecutive additions. If more $FeOAc_2$ was added beyond that point, then we observed an increase in the conductivity, indicating the presence of excess metal ions in solution. A volume of 25 μL contains ~130 μg $FeOAc_2$. The weighing accuracy was determined to be ± 200 μg. The titration method is, therefore, more accurate. The total concentration of Fe-MEPE did not exceed 6 mmol L^{-1}. Alternatively, the required amount of Fe powder is weighed, dissolved in refluxing glacial acetic acid, and added to the ligand dispersed in acetic acid (75 vol %) at room temperature. The solvent was removed under reduced pressure, and the MEPE was isolated as solid powder and stored under inert gas. For the viscosity measurements, the MEPE was directly dissolved in double-distilled water (conductivity < 1 μS cm^{-1}). The deployed acetic acid concentrations were between 78 and 70 vol %. Shear rate, shear viscosity, storage module, and loss module were determined with a double-cylinder dynamic microshear rheometer. Measurements of the kinetic viscosity were performed using a Lauda PVs System equipped with an Ubbelohde capillary. The conductivity of all aqueous (acid) solutions was determined using an inoLab Cond 740P conductometer with an effective range of

Scheme 1. Metal-Ion-Induced Self-Assembly of Metal Ions (Ni(II), Fe(II)) and 1,4-Bis(2,2′:6′,2″-terpyridine-4′-yl)benzene (1) Results in Metallo-Supramolecular Polyelectrolytes (MEPEs)[a]

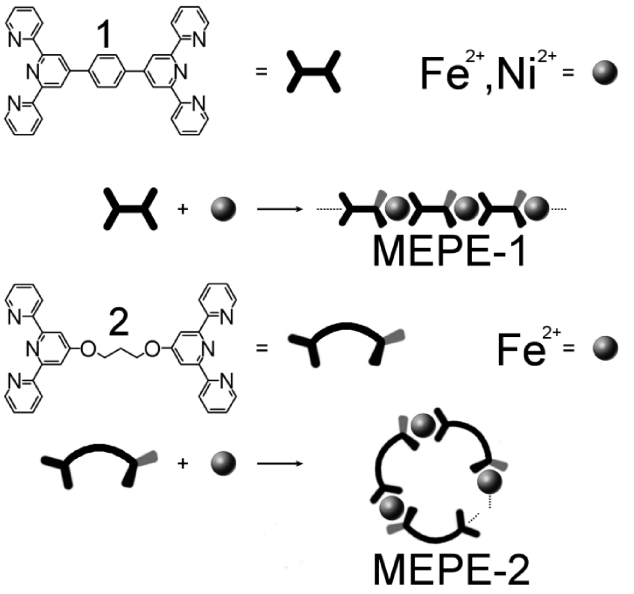

[a] Flexible ligand 1,3-bis[4′-oxa(2,2′:6′,2″-terpyridinyl)]propane (**2**) forms smaller, discrete assemblies, presumably rings with three to four repeat units. The octahedral coordination geometry is indicated by the wedges.

0 μS/cm to 2000 mS/cm and a resolution up to 0.01 μS. For AFM measurements, we used a Veeco Instrument Multimode AFM and Arrow Silica cantilevers in tapping mode with a scan rate of 0.5003 Hz and a scanning area of 3×3 μm.[25] The MEPE solutions were spin coated with a velocity of 5000 rpm on Mica wafers. Small-angle neutron scattering (SANS) measurements were carried out at the SANS II Beamline at the Paul Scherer Institute (Switzerland),[26] providing sufficient counting statistics in a q range of $0.5 \times 10^{-3} \leq q \leq 0.2$ Å^{-1}.[27] The MEPE samples were dissolved in a $[D_2O]/[H_2O] = 0.088$ mixture to minimize solvent scattering. The experiments were carried out with solutions containing a constant ligand concentration of 0.6 mmol L^{-1}. The form factors were calculated using the NIST Center for Neutron Research software (NCNR) available on the web for cylinder-shaped particles.[28] The cylinder length was varied until a best fit of the experimental scattering data was achieved with constant values for the scattering contrast (4.1×10^{-6} Å^2), the volume fraction (0.104), and the MEPE diameter (12 Å). In the range of $0.0001 \leq q \leq 0.001$ Å^{-1}, the experimental scattering intensity deviation was 7%. Fitting the largest and smallest values of each data point gave a variation in the length, L, of 10, 27, and 42 nm.

Results and Discussion

Preparation of MEPE. The MEPEs investigated in the following are prepared by metal-ion-induced self-assembly of the two ditopic ligands 1,4-bis(2,2′:6′,2″-terpyridine-4′-yl)benzene (**1**) and 1,3-bis[4′-oxa(2,2′:6′,2″-terpyridinyl)]-propane (**2**) in aqueous solution with Fe(II) or Ni(II) (Scheme 1). We use the following nomenclature: Fe-MEPE-**1** refers to the assembly made from Fe(II) and ligand **1**. The molecular weight and the properties of MEPEs depend on the experimental parameters that affect the equilibrium, such as concentration and stoichiometry, y, which is the ratio of the concentrations of metal salt, [M], and ligand, [L]. In addition, ligand design also affects the structure and the properties, as we will discuss below.

In a first approximation, the length of the assemblies increases with concentration. However, the maximum length

also depends on the stoichiometry. As soon as one component is consumed in the self-assembly process, growth will terminate, even if the total concentration is increased. We can therefore use the stoichiometry to control the molecular weight of self-assembling polymers. On the other side, the maximum length is realized at exact stoichiometry ([M]/[L] = 1). To fabricate MEPEs in a reproducible and meaningful way, it is of paramount importance to determine the concentration of each component exactly. The simplest procedure is to weigh the components and mix them in solution. However, several sources of error can make this approach unreliable, for example, insufficient purity or unknown composition of the components and weighing errors. Whereas many metal acetates, such as $[Ni(CH_3COO)_2]\cdot 4H_2O$ or $[Zn(CH_3COO)_2]\cdot 2H_2O$, are commercially and at sufficient purity (above 99%) available, Fe(II)-salts are generally not sufficiently pure because of the ease of oxidation of Fe(II) in the presence of weak field ligands. However, acetates are the counterions of choice because the resulting MEPEs exhibit good solubility in water. The ligands are generally air-stable and available with 99% purity and above.

To resolve this critical issue we, therefore, decided to develop a general protocol to assemble MEPEs under reproducible conditions. The method of choice is conductometry because it is readily implemented, provides excellent control in situ, and works essentially for all charged assemblies. In a typical experiment, a known amount of ligand is dissolved in acetic acid, to which a solution containing a known amount of the metal salt is added while the conductivity is monitored.

Figure 1a summarizes the conductivity measurements as a function of the stoichiometry, [M]/[L], for Ni- and Fe-MEPE as well as the neat salts. The Ni(II) and Fe(II) experiments were done in 78 and 75 vol % acetic acid solutions, respectively. Clearly, the conductivity decreases with the addition of $Ni(OAc)_2$ to the ligand solution with a minimum at $[Ni^{2+}]/[L] = 1$ (Figure 1a, circles). The conductivity of neat acetic acid of 200 μS cm^{-1} for 75 vol % and 106 μS cm^{-1} for 78 vol % is considerably lower than that of the acetic acid solution containing the ligand, 331 (75 vol %) and 228 μS cm^{-1} (78 vol %), respectively (Figure 1a). We, therefore, assume that the ligand acts as a base and is protonated, thus contributing to the conductivity. Initially, autodissociated protons, acetate ions, and protonated ligands contribute to the conductivity. As the metal acetate is added, metal-ion coordination of the ligand and subsequent neutralization of the proton under the formation of HOAc reduces the number of charged species. Because of the large binding constants, the metal ions are quantitatively coordinated. As a result, the conductivity decreases in a simple linear fashion with the addition of metal salt to the solution. Apparently, the main contribution is from the conductivity of protons and acetate ions in this concentration window. Because the binding constant K_1 (for $M + L \rightarrow ML$) is much smaller than K_2 (for $L + ML \rightarrow ML_2$), the molar weight of MEPEs is small for $y < 1$.[15,16] Therefore, the contribution of the viscosity to the conductivity can be neglected. Only in the vicinity of $y = 1$, growth proceeds rapidly, and additional effects can contribute to the measurement. Other effects, like ion condensation and ion mobility may also contribute to the conductivity but are not considered here. Above $y > 1$, the conductivity increases because excess ions are added to the solution. We note that the slopes of the left and right branches with respect to $y = 1$ are different. The theory of self-assembly of MEPE predicts that macromolecular species form in the vicinity of $y = 1$, beyond which the molar mass gradually levels off. The

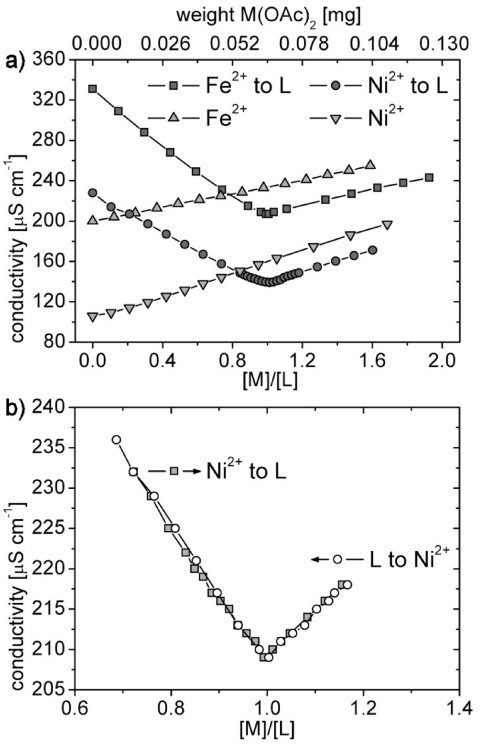

Figure 1. MEPE synthesis under conductometric control. (a) Conductometric titrations of ligand **1** upon addition of $Fe(OAc)_2$ or $Ni(OAc)_2$ (M) in acetic acid solution (squares and circles, respectively) as well as the titration of metal salt to acetic acid without ligand (triangles) as control experiment. (b) Conductivity in the case of forward (squares) and backward (circles) titration of $Ni(OAc)_2$ to ligand **1**. Note that the 1:1 stoichiometry, where maximum chain length occurs, is characterized by a well-defined minimum in the conductivity.

presence of polymeric MEPE, therefore, results in an increased viscosity, thus reducing the conductivity of the solution for $y > 1$. Beyond the 1:1 stoichiometry, the conductivity rises, mainly because of the free excess metal ions. This hypothesis is supported by the observation that the slope of the conductivity of the neat metal salts in acetic acid is very similar to that of the MEPEs (Figure 1a, triangles). Consequently, the minimum in the conductivity at [M]/[L] = 1 coincides with the maximum of the metallo-polyelectrolyte chain length. As for Ni(II) (Figure 1a, circles), we observe the same trend for Fe(II) (squares).

We can experimentally verify the 1:1 stoichiometry by a back-titration. The conductivities of the Ni-to-ligand and ligand-to-Ni titrations are shown in Figure 2b. The excess of metal ions is complexed by the added ligand, which decreases the conductivity due to the formation of MEPE. Both titration curves can be superimposed. With this procedure, we can very precisely adjust the 1:1 point, even if one or both components should be contaminated, of uncertain concentration or composition.

The presented approach to monitor self-assembly of MEPEs by conductometry enables us furthermore to handle oxygen-sensitive metal salts. For $FeOAc_2$, which is very oxygen sensitive in water and in the solid state, we use the following protocol: First, a known amount of iron (powder or filings) is dispersed in glacial acetic acid. Using the procedure outlined in refs 29 and 30, we synthesized a corresponding molar equivalent of $FeOAc_2$. The freshly prepared $FeOAc_2$ solution is directly titrated to the ligand dissolved in acetic acid. As outlined above, the conductivity goes through a minimum as $FeOAc_2$ is added to the ligand.

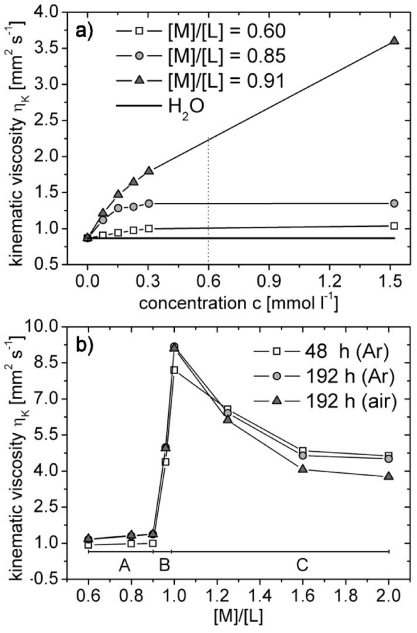

Figure 2. (a) Viscosity of water and different Fe-MEPE solutions with [M]/[L] < 1 as a function of concentration. (b) Viscosity as a function of the [M]/[L] ratio in dependence on time under different environmental conditions. The concentration of the samples is 0.6 mmol L^{-1} (Newtonian regime) and corresponds to the dotted line in part a. See the text for details.

A carefully performed titration makes it possible to determine precisely the minimum and to stop the titration at this point. This is far easier and more exact than any other procedure we tried. Under the conditions described in the Experimental Section, titration steps of 25 μL are adequate to observe a significant change in conductivity. The end point or 1:1 stoichiometry is recognized by the observation that the conductivity does not change for two consecutive additions. Titration errors in the range of two titration steps affect the accuracy of y with ± 0.004 (e.g., [M]/[L] = [1.00 $\pm$ 0.004]/[1]). Now we are in a position to fabricate reproducibly MEPEs with a precisely defined stoichiometry. The Fe-MEPE samples studied below were synthesized following this procedure.

Viscosity of MEPE Solutions. As pointed out above, the molecular mass of MEPEs is a function of concentration and stoichiometry. Because the viscosity is a function of chain length, an increasing viscosity coincides with growing chains. Figure 2a shows the kinematic viscosity, η_K, of Fe-MEPE in H_2O as a function of concentration, c, measured for different [M]/[L] ratios. First, we note that as y approaches 1, the viscosity increases strongly. This is in agreement with predictions from the theory of self-assembly, which states that the molecular weight is small for $y < 1$ and increases as y approaches 1. Also, we see that the viscosity increases with concentration. For small values of y, the viscosity levels off above a concentration of 0.25 mmol L^{-1}. The molecular mass has reached its final value and remains constant above this value. The slope of the viscosity curves, $\partial(\eta_K/c)$, increases as the stoichiometry approaches [M]/[L] = 1, that is as the MEPE chains become longer. Here the final molecular mass has not been reached and is to be found above 1.5 mmol L^{-1}.

Shear viscosity measurements were made to verify if the MEPE solutions are Newtonian fluids (data not shown). In the concentration range from 0 to 0.6 mmol L^{-1}, the MEPE solutions can be considered to be Newtonian fluids. At a concentration of 0.6 mmol L^{-1} and an experimental determined average rod length of 550 nm, at $y = 1$, the average distance between the centers of mass of the rods is 100 nm. The ionic strength of MEPE solution is 1.5 mmol L^{-1}, and the resulting Debye length is 8 nm. Therefore, we assume that under these conditions electrostatic interactions are insignificant, and entanglement of rods is supposed to be negligible. These conclusions are supported by the previously mentioned viscosity data. Above 0.6 mmol L^{-1}, we observe shear thinning; that is, the shear viscosity decreases as a function of shear rate. Also, an alignment of the MEPE rods through the applied shear and disassembly of the MEPE rods into smaller units may contribute to the observed shear thinning.

Figure 2b shows the viscosity as a function of stoichiometry and time within the Newtonian regime. The viscosity data points are an average of three independent measurements; the error of the data points is within the symbols. These measurements demonstrate the high reproducibility of the titration method. The concentration of the ligand is 0.6 mmol L^{-1} for all [M]/[L] ratios, which corresponds to the dotted line in Figure 2a. For $y < 1$ the viscosity is small and almost constant (region A). No macromolecular assemblies are present in this concentration window. As the stoichiometry approaches [M]/[L] = 1 (region B), we note an abrupt increase in the viscosity, indicating the growth of polymers. Above $y > 1$, the viscosity gradually levels off but remains higher than in region A. The viscosity reflects the behavior of the molecular weight as a function of stoichiometry, as predicted for self-assembling polymers.[16] We note that the viscosity, η_K, in Figure 2b is consistent with the viscosity data at 0.6 mmol L^{-1} in Figure 2a (see dotted line) for the corresponding [M]/[L] ratios.

Next, we investigate whether Fe-MEPE is air stable by measuring the viscosity under inert gas (Ar) and under air as a function of time in water. Before the measurements, the MEPE solutions were allowed to equilibrate for 48 h ($t = 0$). At this point, we cannot detect a difference in the viscosity of samples stored and measured under Ar or in air. Therefore, only the data for the measurement under inert gas is shown in Figure 2b. For all samples, the highest viscosity is determined at $y = 1$ (Figure 2b). Considering regions A and B, the viscosity is increasing as a function of time in the period from $t = 0$ to 154 h. Apparently, the Fe-MEPE continues to grow, even after equilibration of 48 h. We note that in this range there is no difference in the viscosity if the sample was stored under air or Ar. Because of the excess of ligand, the Fe(II) is quantitatively complexed by the ligands, forming the air-stable Fe(II)-bis-terpyridine complex.[31] In region C ($y \geq 1$), we observe the same viscosity for the Fe-MEPE under inert gas at $t = 0$ and 154 h. Apparently, the molecular weight of the Fe-MEPE has reached the final molecular mass; the maximum molecular weight in this region is limited by the concentration of the minority component. In contrast, the sample stored and measured under air shows a smaller viscosity as a function of time. Obviously, the oxygen interferes with the equilibrium, for instance the formation of Fe^{3+} may participate in binding thus slightly shifting the equilibrium. For completion, we note that the viscosity of Ni-MEPE solutions in the same stoichiometry range does not change over time because the ligand exchange kinetics of Ni(II) is faster than Fe(II) and is not affected by air because Ni(II) is not air sensitive (not shown).

On the contrary, Fe-MEPE-**2** gives very different results. The viscosity, η_K, of Fe-MEPE-**2** with a concentration of 0.6 mmol L^{-1} at $t = 0$ and $y = 1$ is 0.903 $\pm$ 0.005 mm^2 s^{-1}. This value is low compared with the viscosity of Fe-MEPE-**1** of 8.195 $\pm$ 0.005 mm^2 s^{-1} at the same ratio, concentration,

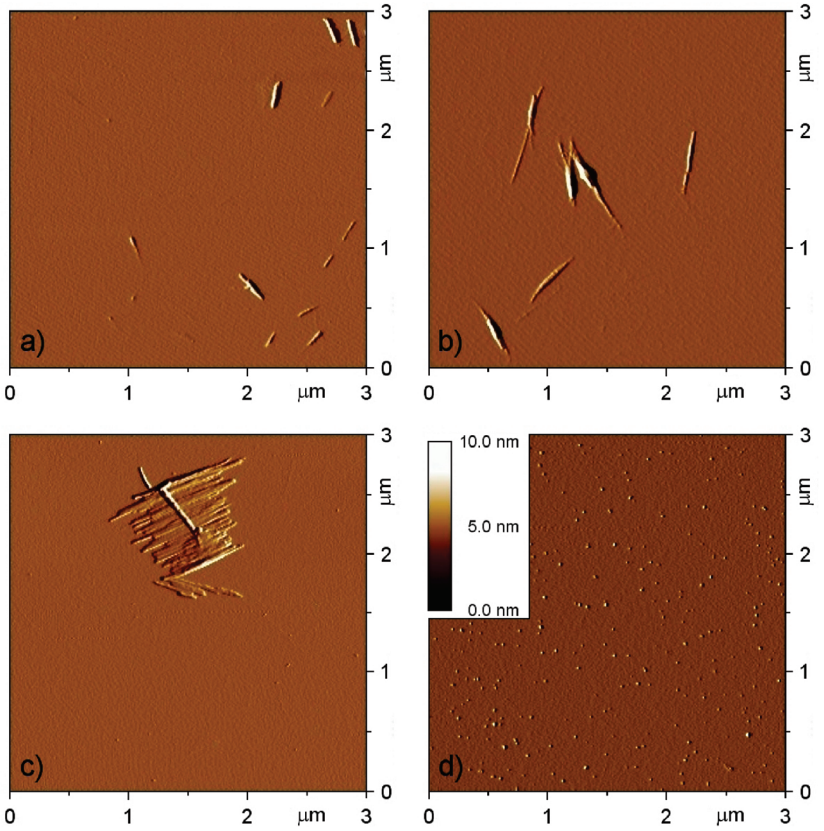

Figure 3. Atomic force microscopy (AFM) images of spin-coated solutions on Fe-MEPE-**1** on mica: (a) [M]/[L] = 0.60, (b) [M]/[L] = 0.85, and (c) [M]/[L] = 0.98 and (d) Fe-MEPE-**2** with [M]/[L] = 1. The corresponding average lengths of the MEPE rods are (a) 150, (b) 320, and (c) 460 nm and (d) the uncorrected average diameter of the Fe-MEPE-**2** dots is 6 nm. The rod diameter is ~1.5 nm.

and equilibration time. With increasing concentration, the viscosity difference between Fe-MEPE-**1** and Fe-MEPE-**2** grows. As for Fe-MEPE-**2**, the viscosity increases only marginally to 0.926 ± 0.005 mm^2 s^{-1} at 1 mmol L^{-1} and 0.962 ± 0.005 mm^2 s^{-1} at 1.5 mmol L^{-1}, whereas the viscosity of Fe-MEPE-**2** reaches 13.96 ± 0.01 mm^2 s^{-1} at 1.5 mmol L^{-1}. The viscosity difference between $y = 0.6$ and 1 is 0.013 ± 0.005 mm^2 s^{-1} for Fe-MEPE-**2** and 7.272 ± 0.005 mm^2 s^{-1} for Fe-MEPE-**1**, respectively. Apparently, the molecular weight of Fe-MEPE-**2** has not increased as y approaches 1. A preliminary study with analytical ultracentrifugation of Fe-MEPE-**2** yields an average number of metal−ligand repeat units (RE) of three to four REs. Considering these results, Fe-MEPE-**2** does not form long polymeric chains or rigid rods like Fe-MEPE-**1** but rather small assemblies, most likely consisting of rings.

Finally, we note that the viscosity of the MEPE-**1** solutions also depends on time. For instance, for a Fe-MEPE-**1** solution ($c = 0.6$ mmol L^{-1}) the viscosity, η_K, increases from approximately 0.93 to 1.32 mm^2 s^{-1} ($y = 0.8$) and 0.97 to 1.52 mm^2 s^{-1} ($y = 0.9$), respectively, within 300 h. In the case of the solution with $y = 0.8$, equilibration takes > 500 h. For the flexible ligand, we do not observe such a time dependence of the MEPE solutions, which supports the hypothesis of ring formation.

Structure of MEPE on a Solid Surface. Using AFM, we can image MEPEs on solid surfaces and estimate their shape and length. The viscosity measurements have shown that equilibration of Fe-MEPE occurs on a time scale of days. Spin-coating occurs on a time scale of seconds to minutes. We, therefore, assume that spin-coating does not significantly change the length of the MEPEs. Whereas interactions of MEPE with the surface cannot be ruled out, AFM imaging of the resulting structures in a series of experiments allows us to observe general trends of the MEPE length as a function of experimental parameters, such as the stoichiometry.

Three Fe-MEPE-**1** solutions with different stoichiometries ($y < 1$) were spin-coated on mica. A representative AFM image is shown in Figure 3. We observe individual or bundles of several straight rods with a height of approximately 1.2 to 1.6 nm, which is in good agreement with the diameter of a single Fe-MEPE-**1** rod of ~1.2 nm.[32] The average length of the rods, where the beginning and end can be unambiguously determined, is 190 ± 20, 395 ± 40, and 600 ± 50 nm for stoichiometries of $y = 0.60$, 0.85, and 0.98, respectively (Figure 3a−c).

An AFM image of Fe-MEPE-**2** on mica is shown in Figure 3d. We observe small spherical objects with heights of ~1.8 nm. On average, the objects are ~6 nm in diameter. Considering the tip−sample convolution, we recognize that the true size is much smaller than this value. The flexible ligand favors the formation of discrete assemblies, most likely rings of three to four repeat units. These results support the viscosity data discussed above and are also in agreement with recent reports by Constable et al.[33] Apparently, ordering effects induced by the interaction of MEPE and the surface are negligible if we compare the AFM images of Fe-MEPE-**1** and Fe-MEPE-**2**. As will be shown in the following section, the rod-like shape of Fe-MEPE-**1** observed on the surface correlates with the solution structure.

Structure of MEPE in Solution. Using SANS, we investigate Fe-MEPE-**1** in deuterated solvent for enhanced contrast to determine the cylinder length. Figure 4a shows the measured SANS patterns for three different stoichiometries. The

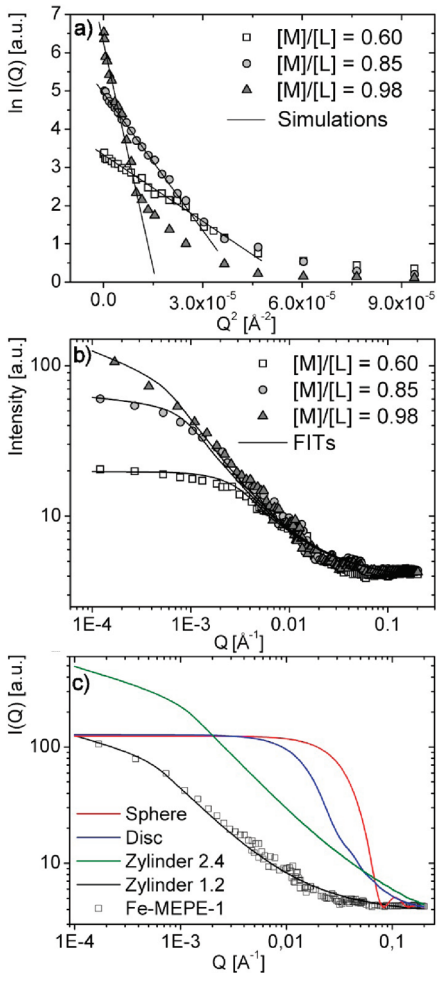

Figure 4. (a) Guinier plots of the neutron scattering data of Fe-MEPE-**1** solutions with [M]/[L] = 0.60, 0.85, and 0.98 (squares, circles, and triangles. For cylindrically shaped particles, the length (U) is given by $U^2 = (12R_G^2 - 1.5d^2)$. The radii of gyration (R_G) are estimated by the linear slope (black lines) of the scattering curve through $\ln[I(q)] = \ln[I(0)] - q^2R_G^2/3R_G$, where d is the MEPE diameter. (b) Scattering intensity (I) as a function of momentum transfer (q) of Fe-MEPE-**1** solutions with [M]/[L] = 0.60, 0.85, and 0.98 (squares, circles, and triangles) recorded using SANS. Computed $I(q)$-curves (black lines) using a form factor for a circular cylinder with uniform scattering length density and length, U, which produced the best fit of the experimental data. The computed lengths U are 138, 380, and 588 nm for [M]/[L] = 0.60, 0.85, and 0.98, respectively. (c) Calculated scattering curves (lines) using a form factor for a circular cylinder 588 nm long and a diameter of d = 1.2 nm (black line) and 2.4 nm (green line). The red and blue lines are computed scattering curves for spherical and disk-shaped particles with the same volume as the above-mentioned cylinder and diameters of 10.8 and 26.8 nm, respectively. Apparently, the cylinder form factor provides the best fit of the experimental scattering data (gray squares).

samples are identical to the ones used for the preparation of AFM images. In the first analysis we apply the Guinier approximation.[34] The radii of gyration (R_G) are estimated by the linear slope of the scattering curve through $\ln[I(q)] = \ln[I(0)] - q^2R_G^2/3$ (Figure 4a) where I is the intensity and q is the transfer momentum. For cylindrically shaped particles, the length (U) is given by $U^2 = (12R_G^2 - 1.5d^2)$ where d is diameter. In the calculations, a diameter of 1.2 nm is used, which corresponds to the diameter of a hypothetical cylinder around a MEPE rod.[22,32] As can be seen from the Guinier equation, the chosen diameter, d, does not significantly affect the final length because $R_G \gg d$. For y equal to 0.60, 0.85, and 0.98, the estimated lengths U are 135, 336, and 546 nm.[35] Considering a length of ~1.5 nm per repeat unit, these values correspond to assemblies of approximately 87, 217, and 352 repeat units. These results are in good agreement with the AFM measurements, which confirms our assumption that the length of Fe-MEPE-**1** does not significantly change during spin coating. Because the Guinier analysis is only valid in the Guinier region $q = 0 \sim 1/R_G$ Å^{-1}, we also apply a second method of analysis.[34,36,37]

In the following, we fit the entire scattering data by calculating the form factor of a monodisperse circular cylinder with uniform scattering length density using the already mentioned diameter, d, of 12 Å. The best fits of the experimental scattering data are achieved with U equal to 138, 380, and 588 nm (Figure 4b). Next, we calculate scattering curves for cylinders of different diameters as well as spheres and discs to estimate the significance of the shape derived from the experimental scattering data. Figure 4c shows the experimental scattering data for Fe-MEPE-**1** (y = 0.98) and the calculated scattering curve for 588 nm long cylinders with diameters of 1.2 and 2.4 nm as well as a sphere (d = 10.8 nm) and a disk (d = 26.8, height 1.2 nm) of the same volume as the cylinder. First, we note that the spheres and discs give a different scattering curve than a rod. Even if the size is changed, the scattering envelope does not fit the experiment scattering intensities. Also, we note that in contrast with the Guinier analysis, the calculated form factor is more sensitive to the diameter of the rod. Increasing the diameter from 1.2 to 2.4 nm alters the entire scattering curve significantly. We can, therefore, conclude that at this concentration the MEPEs exist predominantly as single rods. Overall, these results confirm our hypothesis that self-assembly of rigid ditopic bis-terpyridines results in rodlike macromolecular assemblies in aqueous solution.

Conclusions

In this work on the metal-ion-induced self-assembly of MEPEs, we pursued several objectives: First, we wanted to develop a reliable method to synthesis MEPEs in a reproducible way. This aspect is stimulated by the fact that the molecular weight and, therefore, the macroscopic properties of self-assembling polymers critically depend on the stoichiometry of the components. To provide reproducible results needed for the development of accurate structure−property relationships, a standardized protocol for the preparation of such polymers is presented. The method relies on conductometric titration of the metal ions to the ligand. The particular assembly conditions of MEPEs established here result in a well-defined minimum in the conductivity of the solution at the 1:1 stoichiometry where the maximum chain length occurs. The method allows us to determine unambiguously the stoichiometry and is accurate, reproducible, and easy to use in a laboratory environment. Once the 1:1 stoichiometry is established, every other stoichiometry is readily adjusted by the addition of the appropriate component to the solution. The method is also attractive for air-sensitive metal salts, such as $FeOAc_2$, which is an important advance to previously published procedures because the Fe-MEPE confirms special properties such as spin-crossover.

Second, we study the viscosity of MEPE solutions and could confirm the dependence of the molecular weight on the stoichiometry.[16] The viscosity and, therefore, the molecular weight of MEPE are small for $y < 1$ and increase as y approaches 1. The maximum molar weight occurs at $y = 1$ and decreases gradually for $y > 1$. We note that there is a strong nonlinearity in the viscosity as a function of stoichiometry. This phenomenon is most interesting for the development of smart fluids that can respond to external stimuli. For instance, we could employ electrochemical switching to manipulate the Fe(II) concentration that is the stoichiometry in the vicinity of 1 to control the rheology of the fluid.

And finally, AFM and SANS prove that metal-ion-induced self-assembly of rigid ditopic ligands in aqueous media results in rigid-rod type macromolecular assemblies. Spin-coating of MEPE solutions on a solid surface offers an alternative to investigate the shape and size of MEPE compared with other methods such as analytical ultracentrifugation and scattering methods that are generally more demanding. Under the current conditions, the assemblies reach approximately 500 nm in length corresponding to ~370 repeat units or a molecular weight of ~200 000 g/mol. The flexible ditopic ligand does not form extended macromolecular assemblies, as results from viscosity, AFM, and SANS demonstrate.

Having a reliable protocol at hand and understanding which parameters affect the molecular weight, we are now in a position to study the structure−property relation of these dynamic metallo-supramolecular polyelectrolytes, which will be presented in a forthcoming publication.

Acknowledgment. The scattering experiments were performed at the Swiss spallation neutron source SINQ, Paul Scherrer Institute, Villigen, Switzerland. Neutron measurements were supported by the European Commission under the sixth Framework Program through the Key Action: Strengthening the European Research Area, Research Infrastructures (contract no.: RII3-CT-2003-505925). Funding by DFB is appreciated. We thank Helmuth Möhwald for valuable discussions.

References and Notes

(1) Graber, S.; Doyle, K.; Neuburger, M.; Housecroft, C. E.; Constable, E. C.; Costa, R. D.; Orti, E.; Repetto, D.; Bolink, H. J. *J. Am. Chem. Soc.* **2008**, *130*, 14944–14945.
(2) Maier, A.; Rabindranath, A. R.; Tieke, B. *Chem. Mater.* **2009**, *21*, 3668–3676.
(3) Sato, O. *Acc. Chem. Res.* **2003**, *36*, 692–700.
(4) Weng, W.; Jamieson, A. M.; Rowan, S. J. *Tetrahedron* **2007**, *63*, 7419–7431.
(5) Kersey, F. R.; Loveless, D. M.; Craig, S. L. *J. R. Soc. Interface* **2007**, *4*, 373–380.
(6) Holder, E.; Langeveld, B. M. W.; Schubert, U. S. *Adv. Mater.* **2005**, *17*, 1109–1121.
(7) Bessho, T.; Constable, E. C.; Graetzel, M.; Redondo, A. H.; Housecroft, C. E.; Kylberg, W.; Nazeeruddin, M. K.; Neuburger, M.; Schaffner, S. *Chem. Commun.* **2008**, 3717–3719.
(8) Ruben, M.; Landa, A.; Lörtscher, E.; Riel, H.; Mayor, M.; Görls, H.; Weber, H. B.; Arnold, A.; Evers, F. *Small* **2008**, *4*, 2229–2235.
(9) Johnson, B. F. G.; Kakkar, A. K.; Khan, M. S.; Lewis, J. *J. Organomet. Chem.* **1991**, *409*, C12–C14.
(10) Manners, I. *Angew. Chem., Int. Ed. Engl.* **1996**, *35*, 1602–1621.
(11) Knapp, R.; Schott, A.; Rehahn, M. *Macromolecules* **1996**, *29*, 478–480.
(12) Velten, U.; Rehahn, M. *Chem. Commun.* **1996**, 2639–2640.
(13) Velten, U.; Lahn, B.; Rehahn, M. *Macromol. Chem. Phys.* **1997**, *198*, 2789–2816.
(14) Constable, E. C. *Chem. Soc. Rev.* **2007**, *36*, 246–253.
(15) Holyer, R. H.; Hubbard, I. C. D.; Kettle, S. F. A.; Wilkins, R. G. *Inorg. Chem.* **1966**, *5*, 622–625.
(16) Kurth, D. G.; Higuchi, M. *Soft Matter* **2006**, *2*, 915–927.
(17) Vermonden, T.; vanderGucht, J.; deWaard, P.; Marcelis, A. T. M.; Besseling, N. A. M.; Sudholter, E. J. R.; Fleer, G. J.; CohenStuart, M. A. *Macromolecules* **2003**, *36*, 7035–7044.
(18) Schütte, M.; Kurth, D. G.; Linford, M. R.; Cölfen, H.; Möhwald, H. *Angew. Chem., Int. Ed.* **1998**, *37*, 2891–2893.
(19) Kurth, D. G.; Meister, A.; Thünemann, A. F.; Förster, G. *Langmuir* **2003**, *19*, 4055–4057.
(20) Akcakayiran, D.; Mauder, D.; Hess, C.; K. Sievers, T.; Kurth, D. G.; Shenderovich, I.; Limbach, H.-H.; Findenegg, G. H. *J. Phys. Chem. B* **2008**, *112*, 14637–14647.
(21) Han, F. S.; Higuchi, M.; Kurth, D. G. *J. Am. Chem. Soc.* **2008**, *130*, 2073–2081.
(22) Bodenthin, Y.; Schwarz, G.; Tomkowicz, Z.; Geue, T.; Haase, W.; Pietsch, U.; Kurth, D. G. *J. Am. Chem. Soc.* **2009**, *13*, 2934–2941.
(23) Constable, E. C.; Cargill Thompson, A. M. W. *J. Chem. Soc., Dalton Trans.* **1992**, 3467–3475.
(24) Winter, A.; Berg, A. M. J. v. d.; Hoogenboom, R.; Kickelbick, G.; Schubert, U. S. *Synthesis* **2006**, 2873–2878.
(25) We use tips of type NC-W with characteristics: $T = 4.6\ \mu$m, $W = 45\ \mu$m, $L = 160\ \mu$m, $C = 42$ N/m, and $f_0 = 285$ kHz.
(26) Strunz, P.; Mortensen, K.; Janssen, S. *Phys. B* **2004**, *350*, E783–E786.
(27) In an energy dispersive experiment, the momentum transfer, q, is defind as $q = 2\pi E/hc \sin 2\theta$, where 2θ is the scattering angle, E is the energy, and h and c are Planck's constant and light velocity.
(28) Kline, S.; Munter, A. *Calculate SANS Data on the Web, Particle Model Cylinder*, **1999**. http://www.ncnr.nist.gov/resources/sansmodels/Cylinder.html.
(29) Hardt, H. D.; Möller, W. *Z. Chem.* **1961**, *313*, 57–59.
(30) Welsh, J. Y. U.S. Patent Application 816,927, **1969**.
(31) Han, F. S.; Higuchi, M.; Kurth, D. G. *Adv. Mater.* **2007**, *19*, 3928–3931.
(32) Meister, A.; Förster, G.; Thünemann, A. F.; Kurth, D. G. *ChemPhysChem* **2003**, *4*, 1095–1100.
(33) Constable, E. C.; Harris, K.; Housecroft, C. E.; Neuburger, M.; Schaffner, S. *Chem. Commun.* **2008**, 5360–5362.
(34) Guinier, A.; Fournet, G. *Small-Angle Scattering of X-Rays*; John Wiley and Sons: New York, 1955.
(35) The Guinier radii, R_G, for [M]/[L] = 0.60, 60.85, and 60.98 are 389.386, 968.387, and 1575.1571 Å, and the regression equations are $y = -50586x + 50583$, 53591, $y = -312784x + 312784$, 315939, and $y = -826970x + 312786$, 315735 respectively.
(36) The analysis using the cross section plot $\ln(I(q)\cdot q)$ versus q^2 is not accurate enough because the cylinder-length-to-radius ratio is extremly large.
(37) Glatter, O.; Kratky, O. *Small-Angle X-ray Scattering*; Academic Press: London, 1982.